Applied Physics Express 14, 046502 (2021)
https://doi.org/10.35848/1882-0786/abeb25

LETTER

# Bayesian estimation of equivalent circuit parameters of photovoltaic cells

Kazuya Tada*

*Department of Electrical Materials and Engineering, University of Hyogo, 2167 Shosha, Himeji, Hyogo 671-2280, Japan*

*E-mail: tada@eng.u-hyogo.ac.jp

Received January 21, 2021; revised February 23, 2021; accepted March 1, 2021; published online March 23, 2021

The equivalent circuit model of a photovoltaic cell is useful for understanding device loss mechanisms as well as the design and analysis of systems using photovoltaic cells. Although nonlinear least-squares methods are routinely applied for the extraction of equivalent circuit parameters using current–voltage characteristic curves, they only yield a point estimation sensitive to the initial value and do not provide an estimation error. In this study, a data-driven approach using Bayesian estimation is proposed to extract equivalent circuit parameters. Contrary to the conventional least-squares method, this method does not require tedious initial value adjustments and provides an estimation error.


Photovoltaic power generation successfully ensures access to affordable and clean energy. Moreover, IoT devices such as wireless sensor nodes are becoming increasingly important in the field of big data collection. To avoid the cumbersome task of battery replacement for IoT devices, technologies for energy harvesting from environmental heat, vibration, and light have been developed.[1–4] Among these technologies, indoor photovoltaic cells are promising in situations with a good living environment in terms of energy density.[5–10] The demand for cheaper, environmentally friendly, lighter, and more flexible photovoltaic cells has accelerated the research and development of organic thin-film, dye-sensitized, and perovskite photovoltaic cells. Additionally, dye-sensitized solar cells have been commercialized for indoor photovoltaic applications.[11,12]

The equivalent circuit model of a photovoltaic cell shown in Fig. 1 is useful for understanding the factors responsible for losses and the design and analysis of systems powered by photovoltaic cells. For this reason, it is important to extract equivalent circuit parameters from the current–voltage characteristic curve of a photovoltaic cell, on which many studies have been conducted in the past.[13–18]

Various nonlinear least-squares methods have been proposed for parameter estimation via curve fitting. In these methods, the parameter set is updated by a computational procedure to minimize the error between the estimated values from the theoretical equation and the experimental data. The procedure ends when the update range falls below a specified value. Because it is difficult to distinguish between the global and local minima of the error, the estimated parameter set may stem from a local minimum. Since a different local minimum is obtained that depends on the initial value set, adjusting the initial value set becomes necessary to obtain a good estimation. An inappropriate initial value set does not allow the iteration to converge. Moreover, the least-squares method provides only point estimation and no information on the estimation error. This is problematic considering that the experimental data always contain noise errors.

In recent years, parameter extraction from experimental data via Bayesian estimation has been used in various fields of physics to solve these problems and has yielded significant results.[19–23] In brief, parameter estimations via the least-squares and Bayesian methods can be considered as hypothesis-driven and data-driven approaches, respectively.

Contrary to the least-squares method, Bayesian estimation searches the parameter space according to a pre-specified probability distribution called the prior probability distribution to obtain a probability distribution of the parameter set that can reproduce the experimental data, called the posterior probability distribution. If prior information on the parameters is available, it is possible to set a prior probability distribution using that information. Otherwise, a uniform distribution that includes a theoretically impossible range can be set. Because the result is not a point estimate but a probability distribution, it is possible to calculate the error in the estimated value. This sets Bayesian estimation apart from the conventional least-squares method. As this involves numerical integration in a space with dimensions for several parameters, it is essential to use an efficient algorithm such as the Markov Chain Monte Carlo (MCMC) sampling. In this paper, we report on the Bayesian estimation of equivalent circuit parameters of photovoltaic cells.

We used a software package for Bayesian inference called PyMC3.[24] One of the outstanding features of PyMC3 is its ability to perform Bayesian estimation using an advanced MCMC sampling algorithm called No-U-Turn sampler (NUTS)[25] by simply writing a model code in Python. Therefore, the Bayesian estimation of equivalent circuit parameters can be performed by directly inputting an analytical mathematical expression describing the current–voltage characteristics of the photovoltaic cell. Although the model code is written in Python, PyMC3 internally compiles it in C for a faster calculation.

The current–voltage characteristic of the equivalent circuit model of a photovoltaic cell shown in Fig. 1 is expressed as follows:

$$I = I_s \cdot \left( \exp\left( \frac{V - I \cdot R_s}{n \cdot V_t} \right) - 1 \right) + \frac{V - I \cdot R_s}{R_p} - I_{ph} \quad (1)$$

where $R_s$ and $R_p$ are the series and parallel (shunt) resistances, respectively; $I_s$ and $n$ denote the reverse saturation current and the ideality factor of the diode, respectively; and $I_{ph}$ is the ideal photocurrent. The thermal voltage $V_t$ is approximately 26 mV at room temperature. The expression for current $I$ as a function of voltage $V$ obtained using the principal branch of the Lambert W function (defined as the solution of $W_0(z) \cdot \exp(W_0(z)) = z$) is as follows:[26,27]

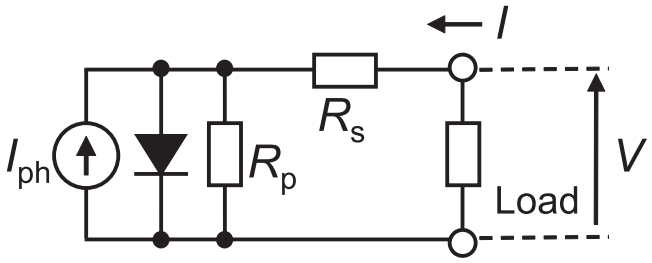


**Fig. 1.** Equivalent circuit model of a photovoltaic cell.

$$I(V) = \frac{n \cdot V_t}{R_s} \cdot W_0(Q(V)) + \frac{V - (I_s + I_{ph}) \cdot R_p}{R_s + R_p} \tag{2}$$

and

$$Q(V) = \frac{I_s \cdot R_s \cdot R_p}{n \cdot V_t \cdot (R_s + R_p)} \cdot \exp\left(\frac{(V + (I_s + I_{ph}) \cdot R_s) \cdot R_p}{n \cdot V_t \cdot (R_s + R_p)}\right) \tag{3}$$

However, this expression tends to deviate from the range of numbers that can be represented by ordinary floating-point systems as it requires the calculation of an exponential function for a large number. Therefore, it is difficult to apply it to the Bayesian estimation using MCMC methods, which ideally explore the entire parameter space.

To overcome this problem, the g function $g(x) = \ln(W_0(\exp(x))) = x - W_0(\exp(x))$ proposed by Roberts[28–30] is used here. We can rewrite Eq. (2) as follows:

$$\begin{aligned} I(V) - \frac{V}{R_s} &= \frac{n \cdot V_t}{R_s} \cdot W_0(Q(V)) - \frac{R_p}{R_s + R_p} \cdot \left(\frac{V}{R_s} + I_s + I_{ph}\right) \\ &= \frac{n \cdot V_t}{R_s} \cdot \left( W_0(\exp(\ln(Q(V)))) \right. \\ &\quad \left. - \ln(Q(V)) + \ln\left(\frac{I_s \cdot R_s \cdot R_p}{n \cdot V_t \cdot (R_s + R_p)}\right)\right) \end{aligned}$$

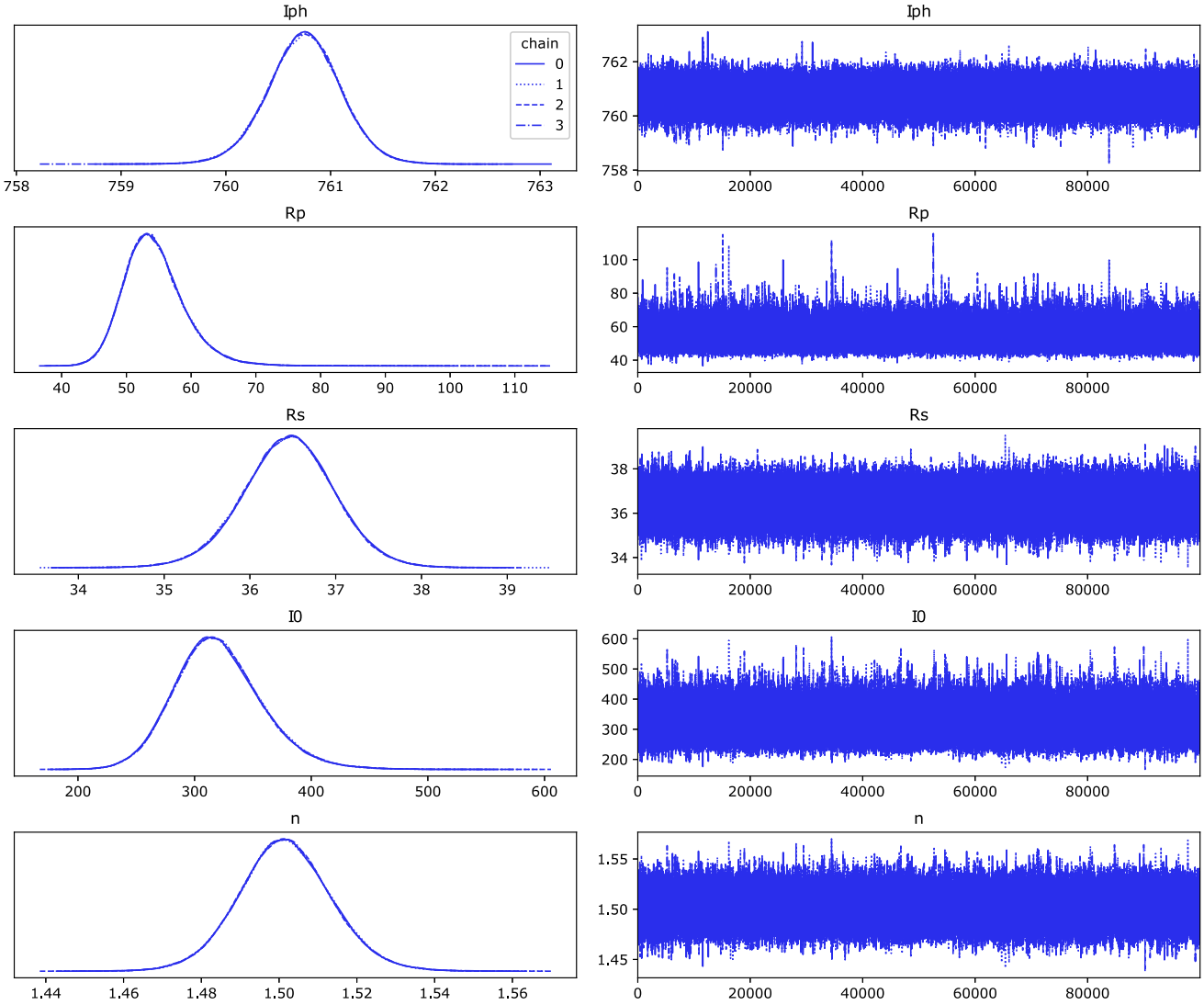


**Fig. 2.** (Color online) Kernel density estimates (left panels) and simulated traces (right panels) for each equivalent circuit parameter of the Si solar cell (R.T.C. France) from Ref. 13.

Thus, we obtain

$$I(V) = \frac{V}{R_s} + \frac{n \cdot V_t}{R_s} \cdot \left( \ln\left( \frac{I_s \cdot R_s \cdot R_p}{n \cdot V_t \cdot (R_s + R_p)} \right) - g(\ln(Q(V))) \right). \quad (4)$$

The calculation algorithm of $g(x)$ using Halley's iteration[28] includes a piecewise function for a rough initial approximation. Unfortunately, this function is difficult to implement in PyMC3, and we need a single analytical expression. After extensive trials, the following formula based on the softplus function was implemented for a rough initial approximation:

$$g_0(x) = \frac{-1}{\ln(1 + \exp(-x))}. \quad (5)$$

Although the iterations in Eq. (5) converge slowly when $x$ is large, it was found that four iterations are sufficient for the range of values used in this study.

In this section, we demonstrate the Bayesian estimation of equivalent circuit parameters using current–voltage characteristics of a Si solar cell.[13] This is chosen because the experimental current–voltage dataset and an estimation by the traditional least-squares method is presented in the reference. As shown below, the prior probability density distributions for each parameter are uniform with a magnitude range of several orders. This means that we do not use any prior information for the estimation. For example, the highest value allowed for $I_{ph}$ was more than ten times the magnitude of the short-circuit photocurrent.

$$I_{ph}[\mathrm{mA}] \sim Unif(1 \times 10^{-2}, 1 \times 10^{4})$$

$$R_p\,[\Omega] \sim Unif(1 \times 10^{0}, 1 \times 10^{5})$$

$$R_s[\mathrm{m}\Omega] \sim Unif(1 \times 10^{0}, 1 \times 10^{8})$$

$$I_s[\mathrm{nA}] \sim Unif(1 \times 10^{-1}, 1 \times 10^{6})$$

$$n \sim Unif(5 \times 10^{-1}, 5 \times 10^{2})$$

The result of the Bayesian estimation performed in the study is shown in Fig. 2. In this study, we employed four chains with 100 000 steps after 10 000 burn-in steps for the estimation. The panels on the left show the smoothed histograms of the marginal posteriors or the kernel density estimates for each variable to be estimated, which are equivalent to the posterior probability distributions. The panels on the right show the sampled values per chain and node throughout the iterations or the simulated traces for each variable to be estimated. The most crucial result obtained by this method is the posterior probability distribution for each parameter, unlike previous studies in which only a point-estimation could be provided. The calculation duration was $3.7 \times 10^4$ s when using PyMC3 installed on a computer with Windows operating system, Intel Core i9 CPU, and approximately 4 GHz clock speed.

The fact that the traces are constantly busily walking around in the right panels is a strong piece of evidence that the MCMC sampling is well performed. Since MCMC sampling is a numerical experiment for a random process, each run/chain returns a unique outcome. Therefore, multiple trials may be required to obtain reasonable traces. However, the central limit theorem states that the probability density function for a sufficient number of samples converges in a normal distribution. Therefore, it is important to have the same profile that mimics the normal distribution for the kernel density estimate in independent chains, as shown in Fig. 2. In some cases, it is necessary to improve the model and change the number of steps for the estimation and burn-in period.

The key outcomes from the Bayesian estimation and the estimation reported in Ref. 13 are listed in Table I. In addition to the mean values, the standard deviations for each parameter, which are not available in previous studies, are also listed. The mean values for each parameter obtained from the Bayesian estimation were very close to the values reported in Ref. 13). As shown in Fig. 3, the simulated curve using the mean values of the estimation gives the experimental current–voltage dataset. The standard deviations were small, indicating that the mean values were accurately estimated. It is worth noting that the present Bayesian estimation was carried out without estimating the appropriate set of initial values, which is indispensable in the conventional least-squares method. Parameter $\widehat{R}$ is used to validate the MCMC sampling. It is estimated that the value of $\widehat{R}$ for all parameters is close to 1.0 if the sampling convergence is good. The deviation of $\widehat{R}$ from 1.0 is usually accompanied by a stagnant trace and skewed kernel density.

Table II shows the Bayesian estimation of the equivalent circuit parameters for the PTB7-Th:$C_{70}$ bulk heterojunction organic photovoltaic cell (OPV) annealed at 175 °C with a power conversion efficiency of 5.64%.[31] The prior probability distribution set in this case is identical to that in the previous example. Kernel density estimates and the simulated traces are shown in Fig. 4. Similar to that in our previous example, the simulated curve using mean values for the estimation gives the accurate experimental current–voltage dataset, as shown in Fig. 5. The value of $n$ is estimated to be approximately 3. Although this value cannot be explained by the simple $p$-$n$ junction diode theory that assumes a single potential drop at the $p$-$n$ junction, a recent study has shown that multiple potential drops within the perovskite photovoltaic cell result in a value of $n$ that is approximately 3.[32] Because the potential profile of bulk heterojunction OPVs is expected to be more similar to that of perovskite solar cells than that of a simple $p$-$n$ junction, the value of $n$ obtained via Bayesian estimation is considered reasonable.

Table III summarizes the effect of noise on the Bayesian estimation of equivalent circuit parameters. The hypothetical current–voltage characteristic corresponding to a relatively

**Table I.** Estimation reported in Ref. 13 and Bayesian estimation of the equivalent circuit parameters of the Si solar cell (R.T.C. France).

| | | Bayesian estimation | | |
|---|---|---|---|---|
| | Ref. 13 | Mean value | Standard deviation | $\widehat{R}$ |
| $I_{ph}$[mA] | 760.8 | 760.7 | 0.4 | 1.0 |
| $R_p$[Ω] | 53.76 | 54.31 | 4.72 | 1.0 |
| $R_s$[mΩ] | 36.4 | 36.45 | 0.54 | 1.0 |
| $I_s$[nA] | 322.3 | 320.5 | 37.9 | 1.0 |
| $n$ | 1.4837 | 1.502 | 0.012 | 1.0 |

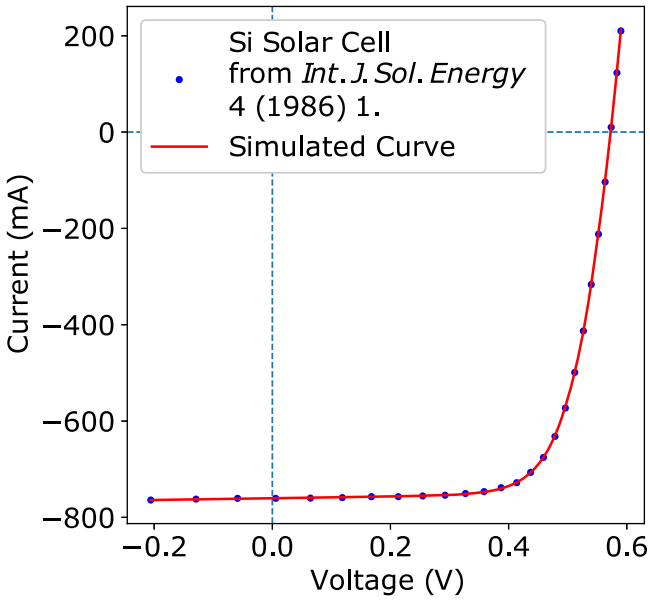


**Fig. 3.** (Color online) Experimental (symbols) and simulated curves (line) for the commercial Si solar cell (R.T.C. France) from Ref. 13.

**Table II.** Bayesian estimation of the equivalent circuit parameters of the OPV (PTB7-Th:C70, annealed at 175 °C) from Ref. 31. *A* denotes the active area of the device.

| | Mean value | Standard deviation | $\widehat{R}$ |
|---|---|---|---|
| $J_{ph}$[mA · cm$^{-2}$] | 14.29 | 0.02 | 1.0 |
| $R_p \cdot A$[Ω · cm$^2$] | 336.7 | 9.6 | 1.0 |
| $R_s \cdot A$[Ω · cm$^2$] | 6.764 | 0.107 | 1.0 |
| $J_s$[nA · cm$^{-2}$] | 580.2 | 124.3 | 1.0 |
| $n$ | 2.871 | 0.061 | 1.0 |

high-performance OPV was calculated from Eq. (4), and the Gaussian noise was added to it. It is observed that increasing the standard deviation of noise by an order of magnitude increases the standard deviations of the estimated parameters by approximately an order of magnitude, while it has a limited effect on their mean values.

In conclusion, this study demonstrated a Bayesian estimation for extracting equivalent circuit parameters of a solar cell. This method does not require tedious initial value adjustments, and the error in the estimation can be obtained using the posterior probability distribution. These are useful

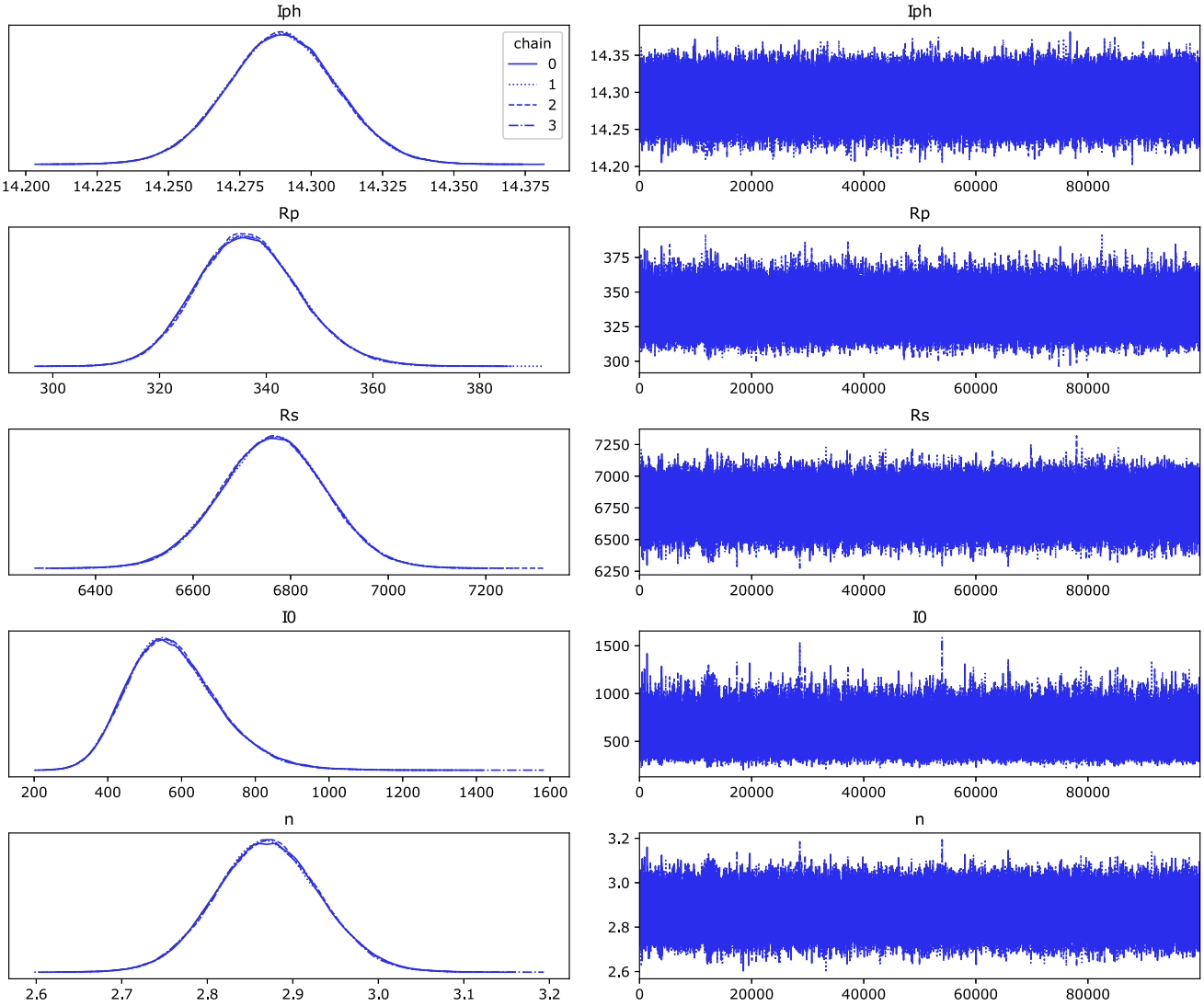


**Fig. 4.** (Color online) Kernel density estimates (left panels) and simulated traces (right panels) for each equivalent circuit parameter of the OPV (PTB7-Th:$C_{70}$, annealed at 175 °C) from Ref. 31.

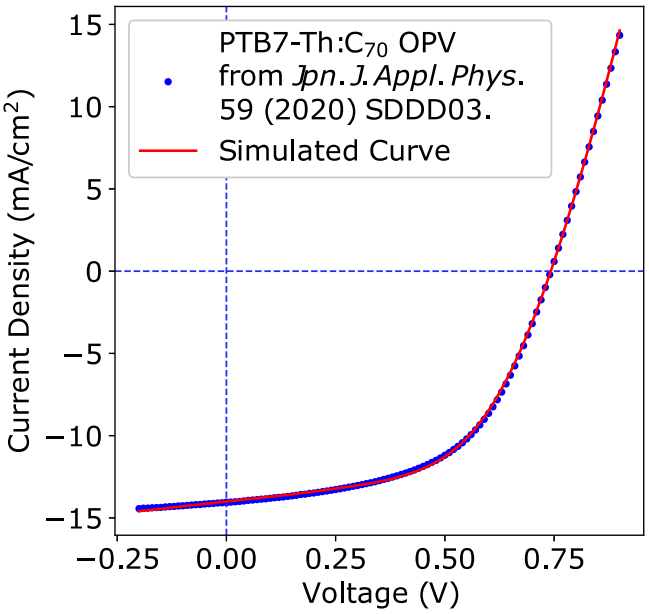


**Fig. 5.** (Color online) Experimental (symbols) and simulated curves (line) for the OPV (PTB7-Th:$C_{70}$, annealed at 175 °C) from Ref. 31.

features that are not found in the conventional least-squares method.

**Acknowledgments** This work was partially supported by JSPS KAKENHI (Grant Number JP18K04241). The author would like to express his gratitude to Prof. Ichiro Akai of Kumamoto University for delivering a highly educational hands-on seminar on data-driven science at University of Hyogo and all those who planned and managed the seminar.

**ORCID iDs** Kazuya Tada https://orcid.org/0000-0001-5697-4048

**Table III.** Effect of Gaussian noise on Bayesian estimation of the equivalent circuit parameters of a hypothetical photovoltaic cell.

| | | $\sigma_{noise} = 0.01$ mA | | $\sigma_{noise} = 0.1$ mA | |
|---|---|---|---|---|---|
| | True value | Mean value | Standard deviation | Mean value | Standard deviation |
| $I_{ph}$[mA] | 16.6 | 16.60 | 0.00 | 16.61 | 0.01 |
| $R_p$[Ω] | 1000 | 992.5 | 5.9 | 944.7 | 53.8 |
| $R_s$[mΩ] | 1000 | 998.8 | 4.5 | 976.6 | 44.8 |
| $I_s$[nA] | 2 | 1.99 | 0.05 | 2.10 | 0.57 |
| $n$ | 1.6 | 1.599 | 0.003 | 1.602 | 0.027 |

1) R. J. M. Vullers, R. van Schaijk, I. Doms, C. Van Hoof, and R. Mertens, Solid-State Electron. **53**, 684 (2009).
2) S. Sudevalayam and P. Kulkarni, IEEE Commun. Surv. Tutor. **13**, 443 (2011).
3) J. W. Matiko, N. J. Grabham, S. P. Beeby, and M. J. Tudor, Meas. Sci. Technol. **25**, 012002 (2014).
4) A. Raj and D. Steingart, J. Electrochem. Soc. **165**, B3130 (2018).
5) I. Mathews, S. N. Kantareddy, T. Buonassisi, and I. M. Peters, Joule **3**, 1415 (2019).
6) A. Sacco, L. Rolle, L. Scaltrito, E. Tresso, and C. F. Pirri, Appl. Energy **102**, 1295 (2013).
7) S. Mori, T. Gotanda, Y. Nakano, M. Saito, K. Todori, and M. Hosoya, Jpn. J. Appl. Phys. **54**, 071602 (2015).
8) H. K. H. Lee, Z. Li, J. R. Durrant, and W. C. Tsoi, Appl. Phys. Lett. **108**, 253301 (2016).
9) K. Tada, Org. Electron. **30**, 289 (2016).
10) K. Tada, Appl. Phys. Express **13**, 024005 (2020).
11) [https://dsc.fujikura.jp/en/] (Accessed: 27 December 2020).
12) [https://industry.ricoh.com/en/dye-sensitized-solar-cell/] (Accessed: 27 December 2020).
13) T. Easwarakhanthan, J. Bottin, I. Bouhouch, and C. Boutrit, Int. J. Sol. Energy **4**, 1 (1986).
14) A. M. Humada, M. Hojabri, S. Mekhilef, and H. M. Hamada, Renew. Sustain. Energy Rev. **56**, 494 (2016).
15) Y. Li, W. Huang, H. Huang, C. Hewitt, Y. Chen, G. Fang, and D. L. Carroll, Sol. Energy **90**, 51 (2013).
16) J. A. Jervase, H. Bourdoucen, and A. Al-Lawati, Meas. Sci. Technol. **12**, 1922 (2001).
17) K. Nishida, M. Oka, H. Hase, and H. Naito, IEEJ Trans. EIS **131**, 283 (2011) [in Japanese].
18) K. Tada, Phys. Status Solidi A **215**, 18004 (2018).
19) K. Nagata, S. Sugita, and M. Okada, Neural Netw. **28**, 82 (2012).
20) R. E. Brandt, R. C. Kurchin, V. Steinmann, D. Kitchaev, C. Roat, S. Levcenco, G. Ceder, T. Unold, and T. Buonassisi, Joule **1**, 843 (2017).
21) I. Akai, K. Iwamitsu, and M. Okada, J. Phys. Conf. Ser. **1036**, 012022. (2018).
22) K. Iwamitsu, M. Okada, and I. Akai, J. Phys. Soc. Jpn. **89**, 104004 (2020).
23) I. Sakata, Y. Nagano, Y. Igarashi, S. Murata, K. Mizoguchi, I. Akai, and M. Okada, Sci. Tech. Adv. Mater. **21**, 67 (2020).
24) J. Salvatier, T. V. Wiecki, and C. Fonnesbeck, PeerJ Comput. Sci. **2**, e55 (2016).
25) M. D. Hoffman and A. Gelman, J. Mach. Learn. Res. **15**, 1593 (2014).
26) A. Jain and A. Kapoor, Sol. Energy Mater. Sol. Cells **81**, 269 (2004).
27) R. M. Corless, G. H. Gonnet, D. E. G. Hare, D. J. Jeffrey, and D. E. Knuth, Adv. Comp. Math. **5**, 329 (1996).
28) K. Roberts, (2015), (arXiv:1504.01964v1).
29) K. Roberts and S. R. Valluri, (2015), (arXiv:1601.02679v1).
30) K. Tada, IEEJ Trans. Electr. Erectron. Eng. **14**, 333 (2019).
31) K. Tada, Jpn. J. Appl. Phys. **59**, SDDD03 (2020).
32) N. E. Courtier, Phys. Rev. Appl. **14**, 024031 (2020).